On the Theory of Space Charge Between Parallel Plane Electrodes

By C. E. FAY, A. L. SAMUEL and W. SHOCKLEY

The problem of the potential distribution, current, and electron transit time resulting from the perpendicular injection of electrons into the space between parallel planes is considered. The electrons are assumed to be injected uniformly with velocities corresponding to the potential of the plane through which they are injected. Consideration of all possible solutions of the basic equation shows that four general types of potential distribution are possible. Curves are given which enable the easy calculation of transmitted current and transit time and show the complete potential distribution for any concrete example. The case for current injected through both planes is also considered.

The complete mathematical treatment is given in the appendix.

SPACE charge has been studied extensively since the publication of the first papers on the subject by Child [1] in 1911 and Langmuir [2] in 1913. These papers in common with many which followed [3, 4, 5, 6, 7] dealt for the most part with potential distributions which occur when electrons are injected into a region with relatively small initial velocities.

The problem of space charge between parallel planes when the electrons possess arbitrary initial velocities, although contained implicitly in some of this early work, was first considered in detail by Gill [8] in 1925. Gill appears to have clearly understood the phenomenon but did not publish a complete analysis. Other workers, beginning with Tonks [9] in 1927, have considered various aspects of the problem,[10, 11] and recently Plato, Kleen, and Rothe [12, 13] published an extensive analysis. They did not include transit time calculations and their published curves are not easily adaptable for numerical

[1] C. D. Child, *Phys Rev.*, **32**, 492 (1911).
[2] I. Langmuir, *Phys. Rev.*, **2**, 450–486 (1913); also *Phys. Zeits*, **15**, 348 (1914).
[3] W. Schottky, *Phys. Zeits*, **15**, 526 and 624 (1914).
[4] P. S. Epstein, *Vehr. d.D. Phys. Ges.*, **21**, 85 (1919).
[5] T. C. Fry, *Phys. Rev.*, **17**, 441 (1921); *Phys. Rev.*, **22**, 445 (1923).
[6] I. Langmuir, *Phys. Rev.*, **21**, 419 (1923).
[7] I. Langmuir and K. B. Blodgett, *Phys. Rev.*, **22**, 347 (1923); *Phys. Rev.*, **24**, 49 (1924).
[8] E. W. B. Gill, *Phil. Mag.*, **49**, 993 (1925); *Phil. Mag.*, **10**, 134 (1930).
[9] L. Tonks, *Phys. Rev.*, **30**, 501 (1927).
[10] H. C. Calpine, *Wireless Engineer*, **13**, 473 (1936).
[11] Myers, Hartree and Porter, *Proc. Roy. Soc.* **158**, 23 (Jan. 1937).
[12] G. Plato, W. Keen, and H. Rothe, *Zeit. f. Phys.*, **101**, 509 (July 1936).
[13] H. Rothe and W. Keen, *Telefunken Rohre* No. 9 (April 1937).

calculations. In this country Salzberg and Haeff [14] have presented a solution, apparently quite complete, which has not as yet been published. The present independently derived solution differs from other published work in the manner of presentation and in an attempt at completeness. The results are presented in the form of curves which give potential distributions, electron transit times, and current-voltage relations, directly in terms of units which have a simple physical significance.

Statement of the Problem

In common with some of the earlier treatments, the present discussion will be restricted to a consideration of the steady state potential distributions which can exist in an evacuated region between two parallel planes at known potentials when electrons having normal velocities corresponding to these potentials are injected into the region through one or both planes. For definiteness the case in which all of the current is injected through one plane will be considered first. It will then be shown that the results may be applied to the more general problem. It is supposed that the electrostatic potential is a function of one rectilinear coordinate only and that all the electrons move parallel to this coordinate and have the same total energy. The assumption of equal energy electrons leads to indeterminancy at planes where the potential and its gradient are both zero. At these planes the existence of non-uniform electron velocities will be recognized in so far as it provides a selective mechanism to resolve the mathematical indeterminancy.[15]

Units

It has been found convenient to express voltages, currents, distances and transit times in terms of some derived units which are related to these quantities in certain ways by the simple Child's law equation for space charge limited current and by the corresponding transit time equation. The use of such derived units makes it possible to present a limited number of curves which are then applicable to a wide variety of conditions and may be used with a minimum amount of computations. The physical significance of the units also simplifies the interpretation of the results.

In order to understand how these units are obtained consider the hypothetical situation shown in Fig. 1 in which an electron current from a space charge limited cathode is injected into the region to the

[14] B. Salzberg and A. V. Haeff, *Proc. I.R.E.*, 25, 546 (May 1937).—Abstract only. This paper appears in full in the January 1938 issue of the *R.C.A. Review.*

[15] This procedure has been justified by Langmuir. See *Reviews of Modern Physics*, vol. 3, pp. 237–244 (1931).

right of a plane at a potential V_1.[16] From Child's equation the current in amperes per square centimeter is given by

$$I = 2.33 \times 10^{-6} \frac{V_1^{3/2}}{S_0^2} = \frac{a^2 V_1^{3/2}}{S_0^2} \text{ (amps. per sq. cm.)} \qquad (1)$$

or solving for S_0

$$S_0 = 1.527 \times 10^{-3} \frac{V_1^{3/4}}{I^{1/2}} = \frac{a V_1^{3/4}}{I^{1/2}} \text{ (centimeters).} \qquad (2)$$

Accordingly, whenever the conditions at the first plane are represented

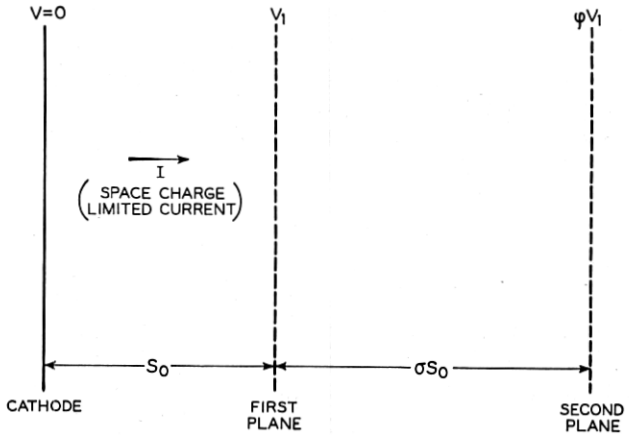

Fig. 1—Hypothetical conditions to assist in visualizing the unit of distance S_0.

by I and V_1, distance from the first plane may be measured in units of S_0. The distance in centimeters is then

$$S = \sigma S_0. \qquad (3)$$

Similarly a natural unit of potential is V_1 and the potential of any plane at a distance S is then given by

$$V = \varphi V_1. \qquad (4)$$

Potential Distributions

All possible potential distributions to the right of the first plane can now be expressed in terms of φ as a function of σ. The mathematical derivation is straightforward and is given in the appendix.

[16] This analogy is useful in getting a physical picture of the units but it must not be carried too far as will be evident when the problem of reflected currents is considered.

The results are shown in Figs. 2, 3 and 4. Figures 6 to 11 refer to current voltage relationships discussed in a later section.

To find the potential distribution when a second plane at a distance σ away from the first plane is held at a potential φ, one enters the figures with the values of φ and σ. Any member of the family of curves drawn in heavy solid lines passing through this point represents a possible potential distribution. The regions occupied by the heavy curves are bounded by certain limiting curves identified by lower case letters. These curves correspond to certain space charge conditions between the planes and are indicated by the same letter whenever met. The dashed curves refer to transit time and are explained below. Situations corresponding to low potentials and large spacings occur, for the most part, on Fig. 2, while those for high potentials and small spacings occur on Fig. 3. An overlap region exists for which potential distributions may be found on both families of curves. The interpretation of this is found by inquiring more closely into the nature of the curves of Figs. 2, 3 and 4.

There are in all four distinct types of potential distributions. These are:

Type *A*—The second plane is at a negative potential. All the injected current is reflected. Potential distributions are the same as for the case of temperature limited emission with the current $2I$ from the zero potential plane.

Type B—Both planes positive with potential zero between them. Injected current partially transmitted and partially reflected. Potential distributions corresponding to space charge limited emission on both sides of a virtual cathode at the zero of potential.

Type C—Both planes positive with a potential minimum (at a positive potential) between them. Complete transmission of injected current.

Type D—Both planes positive with no minimum between them. Complete transmission of injected current.

The curves on Fig. 2 are seen to fall into two groups, those which extend to negative values of φ (marked with values of β) and those which contain the value $\varphi = 0$ but which remain positive. The first group (Type A) obviously corresponds to conditions under which all of the injected current returns to the first plane. The slopes of these potential curves at the reflection planes are not zero but are related to the parameter β (shown on the curves) by the equation

$$\frac{d\varphi}{d\sigma} = -\frac{4}{3}\sqrt{2}\beta^{1/4}. \tag{5}$$

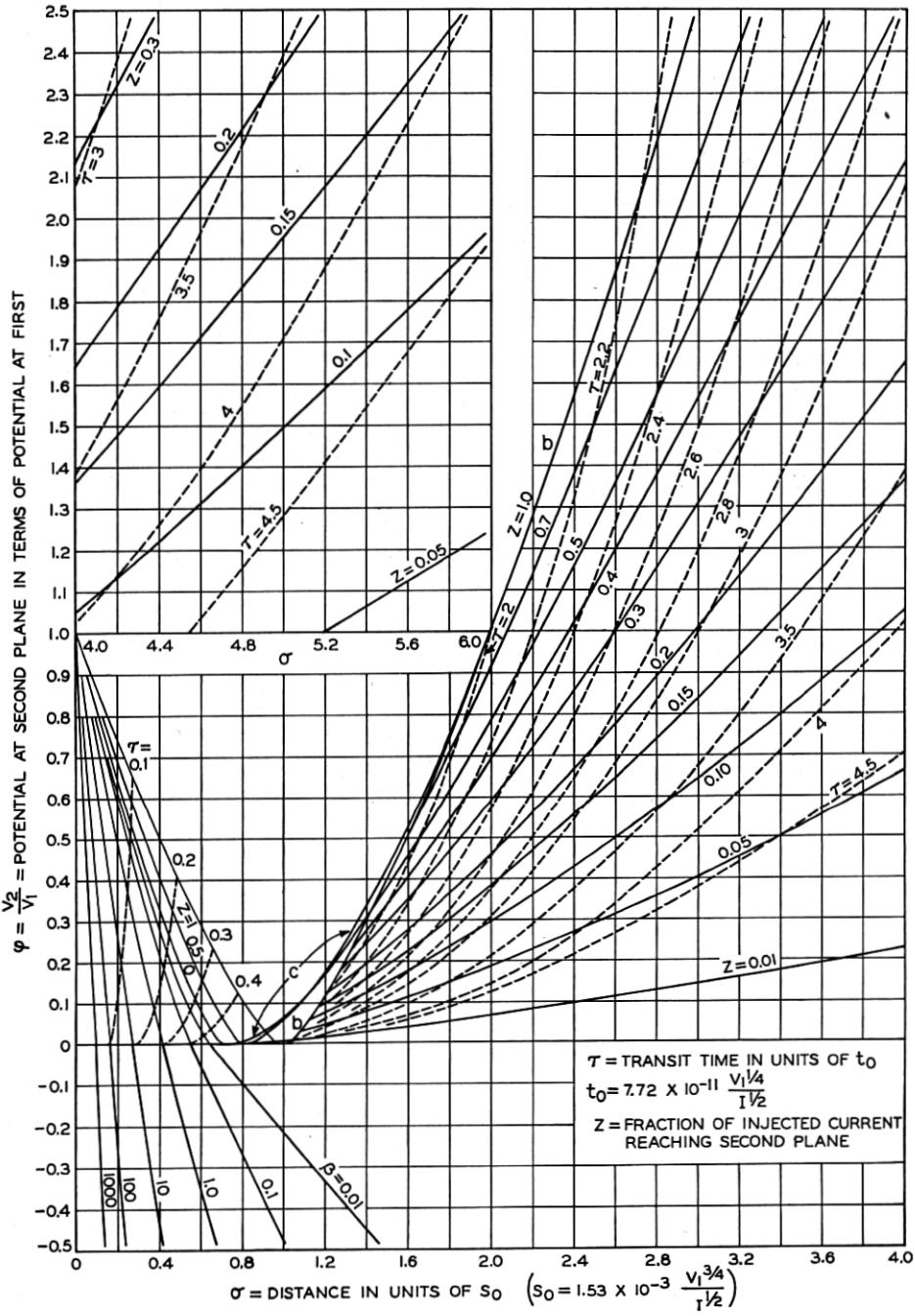

Fig. 2—Potential distributions of the A and B types. The solid lines are the potential curves; the broken lines indicate the transit times.

For the second group of curves (Type B) a certain fraction of the current denoted by Z (and so indicated on the curves) will be transmitted while the fraction $1 - Z$ will be reflected toward the first plane. These potential curves have zero slopes at the reflection planes so that they correspond to solutions of Child's equation on both sides of a so-called virtual cathode existing at the reflection plane. For each value of Z from 0 to 1 a possible potential distribution is obtained.

It will be observed that the portions of the solid curves to the left of the zero points are drawn lighter than the rest. These portions correspond to potential distributions resulting from conditions with reflected current and so while applying as extensions of the heavy curves to the right they cannot be entered directly with values of φ and σ. Should values used to enter the figure fall in this region the absence of a potential zero is indicated and the correct distribution is obtained by entering Fig. 3. Before leaving Fig. 2 the existence should be noted of a small domain lying between the curves marked b and c for which two different B solutions are possible for the same injected current, spacing, and potential, one corresponding to larger values of Z than the other. The significance of this region will be apparent when the current voltage relationships are considered. All solutions of the A and B types are represented on Fig. 2.

Solutions of the C and D types are to be found on Fig. 3 except for a small overlap region which for clearness is shown on Fig. 4. Values of φ and σ which cannot be entered on Fig. 2 as well as values common to both B and C types are to be found on these figures. The additional overlap solutions of the C type are shown in Fig. 4. These are extensions of the potential distribution curves of Fig. 3 after they reach the right-hand boundary curve where they turn inward as shown and overlap the other solutions.

For convenience each curve of the C type is labeled by the value of its minimum potential. The parameters of the D curves do not have this simple physical significance. However, for all cases the value of the curve parameter is simply related to the electric field at the first plane by the equations:

type C
$$\frac{d\varphi}{d\sigma} = -\frac{4}{3}\sqrt{1 - \varphi_{min.}}^{1/2}. \tag{6}$$

type D
$$\begin{cases} \dfrac{d\varphi}{d\sigma} = \dfrac{4}{3}\sqrt{1 - \alpha^{1/2}}, & (7) \\ \dfrac{d\varphi}{d\sigma} = \pm\dfrac{4}{3}\sqrt{1 + \beta^{1/2}}. & (8) \end{cases}$$

type A
$$\frac{d\varphi}{d\sigma} = -\frac{4\sqrt{2}}{3}\sqrt{1 + \beta^{1/2}}. \tag{9}$$

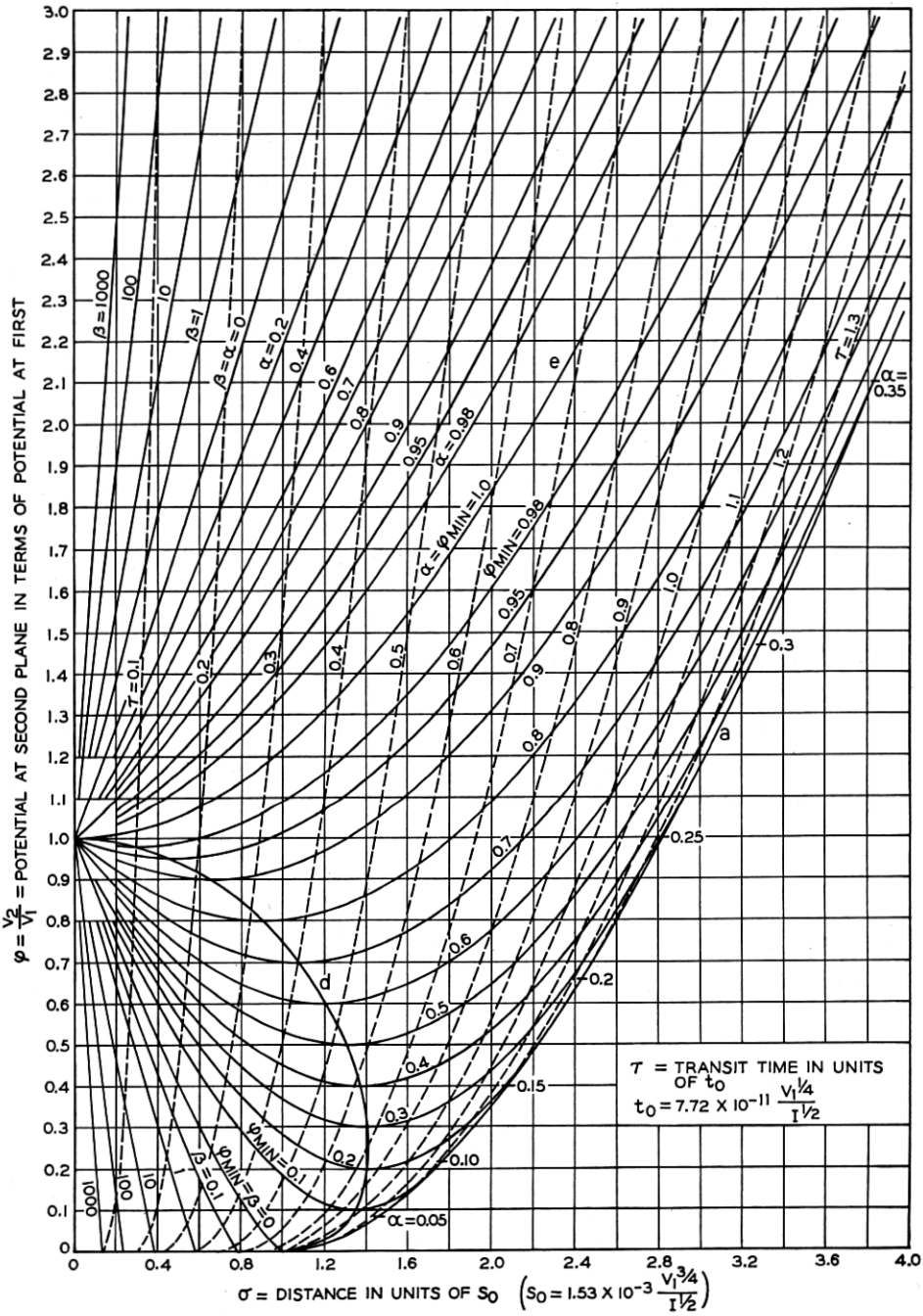

Fig. 3—Potential distributions of the C and D types. The solid lines are potential curves, the broken lines indicate the transit times.

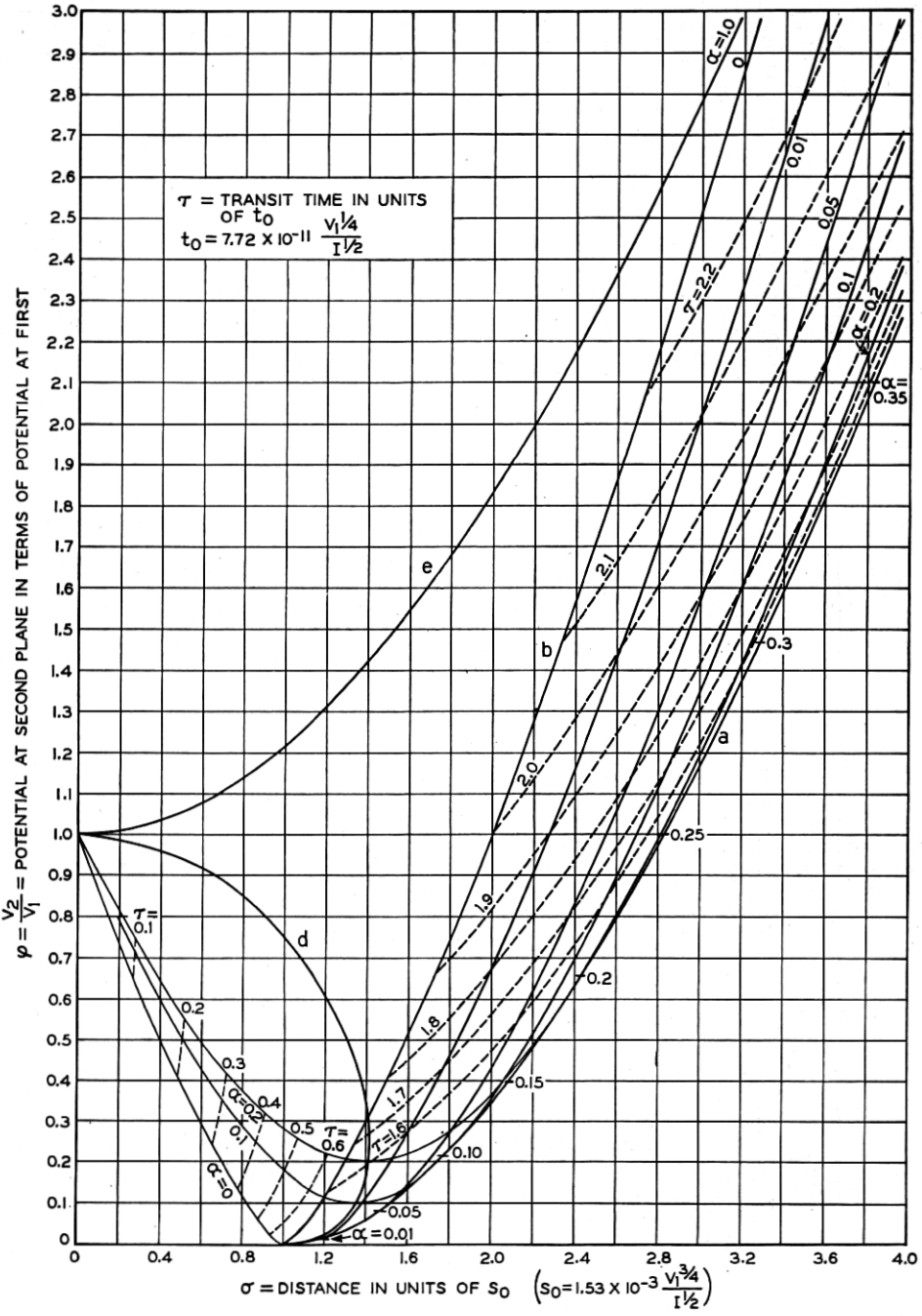

Fig. 4—Potential distributions of the C overlap type.

It should be noted that while some of the curves in the D region shown in Fig. 3 resemble the portions of the curves drawn in light lines on Fig. 2, the curves in Fig. 3 have essentially different physical content, representing solutions in which all of the injected current is transmitted. Values of σ and φ may, therefore, be entered in all regions on Fig. 3 while entering values on Fig. 2 are restricted to the regions covered by the heavy lines.

The occurrence of overlap regions indicates that for certain boundary conditions more than one type of potential distribution may exist. In the practical case the choice between these various possible solutions depends upon the manner in which the boundary conditions are established.[17]

Current Injection from Both Sides

The present analysis although derived on the assumption of current injection from one side only is equally applicable to the situation shown schematically in Fig. 5. The potential distribution curves

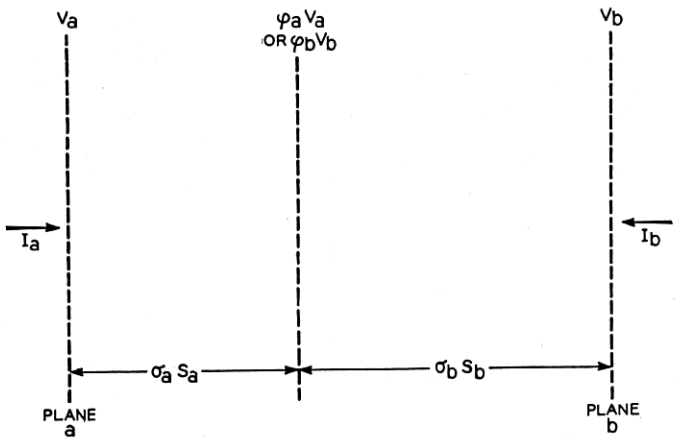

Fig. 5—Schematic representation of the general conditions under which the potential distribution analysis may be applied.

which occur when the currents I_a and I_b are injected from opposite sides will be identical with those obtained for an assumed injection from one side only of a current I equal to the numerical sum of I_a and I_b. Values of V_1, φ and σ are chosen to correspond with an assumed direction of injection and these values are entered on the figures. For solutions of the B type, different distributions will result depending

[17] This matter will be treated in more detail in the section on circuit characteristics.

upon the assumed direction of I. In some instances all solutions may correspond to physically realizable distributions for the double injection case. The solutions will, in general, require that the potential zero be located at different places and may require that the net flow of current across the zero plane be in opposite directions. The physical reality of each of these distributions must be checked by noting the value of Z for the indicated solution and solving for the derived current $(2 - Z)I$ on the injected side of the zero potential plane and the derived transmitted current ZI. If these are respectively greater than the numerical values of I_a and I_b (paired consistent with the assumed direction of injection) the indicated solution is possible. In addition there may exist a solution in which the currents I_a and I_b are each totally reflected at two different zero potential planes, separated by a region of zero potential. The possible existence of this solution must be tested for separately.

Electron Transit Time

So far no use has been made of the dashed curves shown in Figs. 2, 3 and 4. These give the electron transit time from the first plane to any desired plane. The significance of the unit of time is to be found by again referring to Fig. I. The time an electron takes to travel from the cathode to the first plane is given by

$$t_0 = c\frac{V_1^{1/4}}{I^{1/2}} = 7.72 \times 10^{-11}\frac{V_1^{1/4}}{I^{1/2}} \text{ (seconds)}. \tag{10}$$

This value of t_0 is a natural unit of time to be used whenever the conditions at the first plane are expressed by V_1 and I just as S_0 is a natural unit of distance. Accordingly, electron transit times from this plane to any other plane are expressed in units of t_0. The time in seconds is then

$$T = \tau t_0. \tag{11}$$

Transit times for reflected electrons are not given but may be computed by taking the time to the reflection plane and adding to it the returning time. This latter is obtained by taking the difference between the time to the reflection plane and the direct time to the plane under consideration.

Circuit Characteristics

In many practical cases the first plane will coincide with a mesh or grid electrode in a vacuum tube and the second plane will correspond with a plate electrode. Under these conditions the current-voltage

relations which exist at the second plane are of considerable interest. Since the distance between the planes is now fixed, the parameter σ is not appropriate. However, the spacing d between planes and the voltage V_1 serve to define a natural unit of current density i_0, which is indicated by the hypothetical situation of Fig. 6. The value of i_0 is

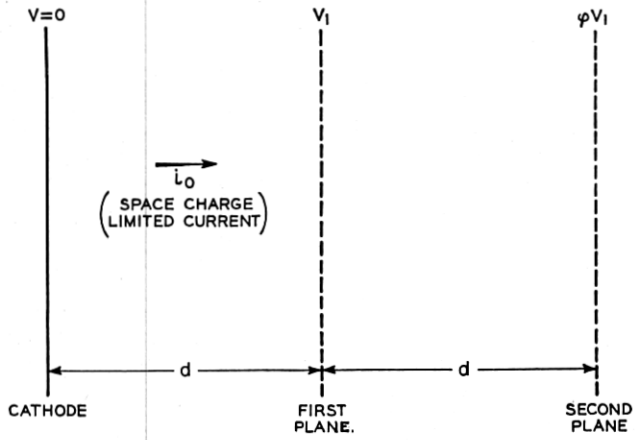

Fig. 6—Hypothetical conditions to illustrate the significance of the unit of current i_0.

$$i_0 = a^2 \frac{V_0^{3/2}}{d^2} = 2.33 \times 10^{-6} \frac{V_1^{3/2}}{d^2} \text{ (amperes per sq. cm.)} \qquad (12)$$

The current in units of i_0 is denoted by γ so that the injected current I in amperes per sq. cm. is given by

$$I = \gamma i_0. \qquad (13)$$

Similarly, the transmitted current under conditions corresponding to type B potential distributions will be

$$ZI = Z\gamma i_0. \qquad (14)$$

Specifying γ and φ is equivalent to specifying σ and φ.[18] For this reason many of the limiting curves of the circuit characteristic plots are simply related to those shown in the potential distribution plots and are designated by the same letters. The regions for which the different types of potential distributions may exist are shown in Fig. 7 now in terms of γ and φ. In Fig. 8 the regions are defined in terms of φ and the transmitted current $Z\gamma$. The boundaries of the C and D

[18] This is a consequence of the relationship $\gamma = \sigma^2$, which is derived in the appendix.

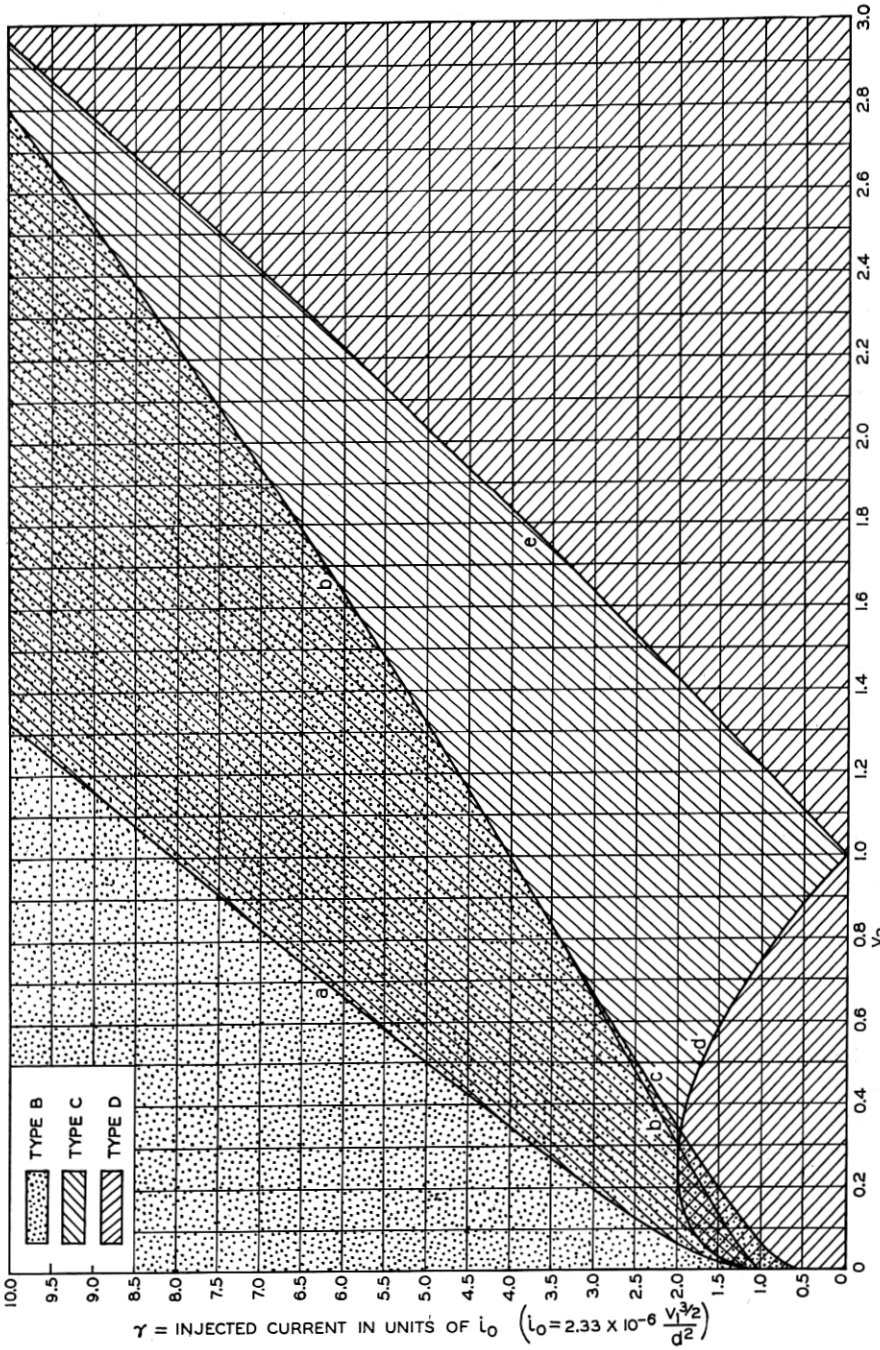

Fig. 7—Key chart giving boundary conditions for the different distributions in terms of the potential and the injected current.

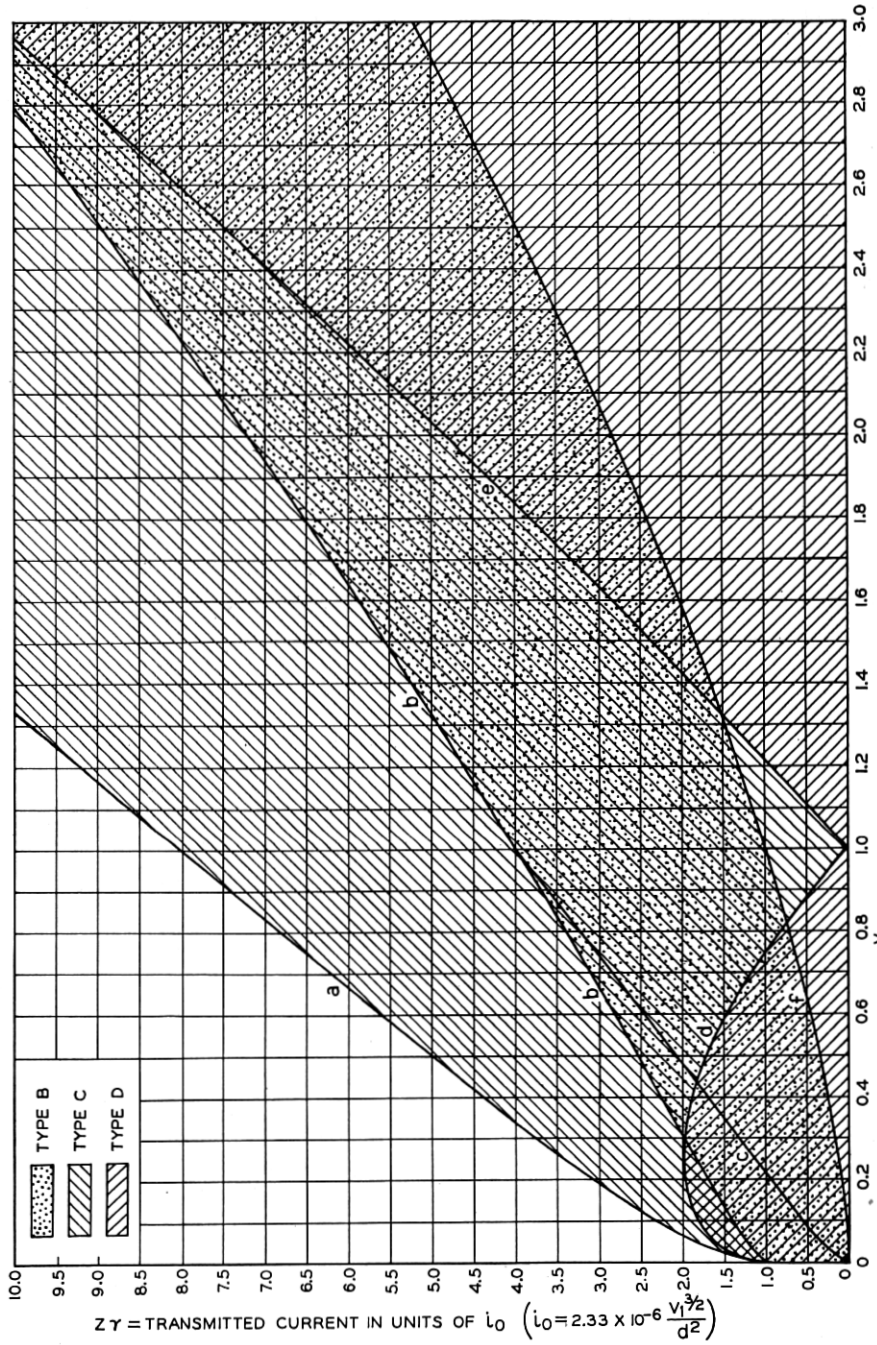

Fig. 8—Key chart giving boundary conditions for the different distributions in terms of the potential and the transmitted current.

regions are of course the same in the two plots (i.e., $Z = 1$) while the boundaries of the B region are changed, since only the portion $Z\gamma$ of the injected current is transmitted. The A region, which corresponds to negative values of φ for all values of γ and gives $Z\gamma = 0$, is not indicated. It may be of interest to note that for any given value of φ it is impossible to transmit more than a certain maximum current, shown by curve a, and that this maximum occurs for a C type distribution. For injected currents greater than this amount only type B distributions are possible.

An enlargment of the B region is shown in Fig. 9a and a portion of the region to a still larger scale in Fig. 9b. Lines for constant injected current γ are plotted with the potential φ and the transmitted current $Z\gamma$ as the coordinates. These plots correspond to plots frequently used to describe vacuum tube characteristics and may be used accordingly. For values of γ less than four and values of φ less than unity, double values of $Z\gamma$ appear. In the region lying between the lines b and c on Fig. 9, the slopes of the constant γ lines are negative corresponding to conditions which are unstable unless sufficient resistance is included in the external circuit. Conditions outside of this region are always stable and need no further comment.

Solutions of the C type are shown in Fig. 10a. For these solutions the injected and transmitted currents are equal. The depth of the potential minimum between the two planes is, however, of interest and is shown in the figure in terms of the lesser of the two boundary potentials. For values of φ greater than unity the value of φ min. (i.e., the minimum potential in units of V_1) is indicated while for values of φ less than unity the value of $\varphi_{min.}$ (i.e., the minimum potential in units of V_2) is shown. In the enlargement, Fig. 10b, both values are given. For values of $\varphi_{min.} = 1$, curve e, and $\varphi_{min.} = 1$, curve d, the potential minimum is equal to the potential at one of the planes and is located at this plane. For currents greater than the value indicated by these limiting curves the potential minimum becomes deeper and moves away from the plane while for lesser currents it disappears entirely. The minimum value to which the potential may be forced by increasing the injected current before the distribution changes precipitously to one of the B type is indicated by the values on curve a.

Again to avoid confusion the overlap type C region is shown separately in Fig. 11. Conditions are somewhat different for this region in that with any assumed value of φ a minimum potential of 0 (but with complete transmission of injected current) occurs for a certain value of γ. With increasing injected current, the potential minimum

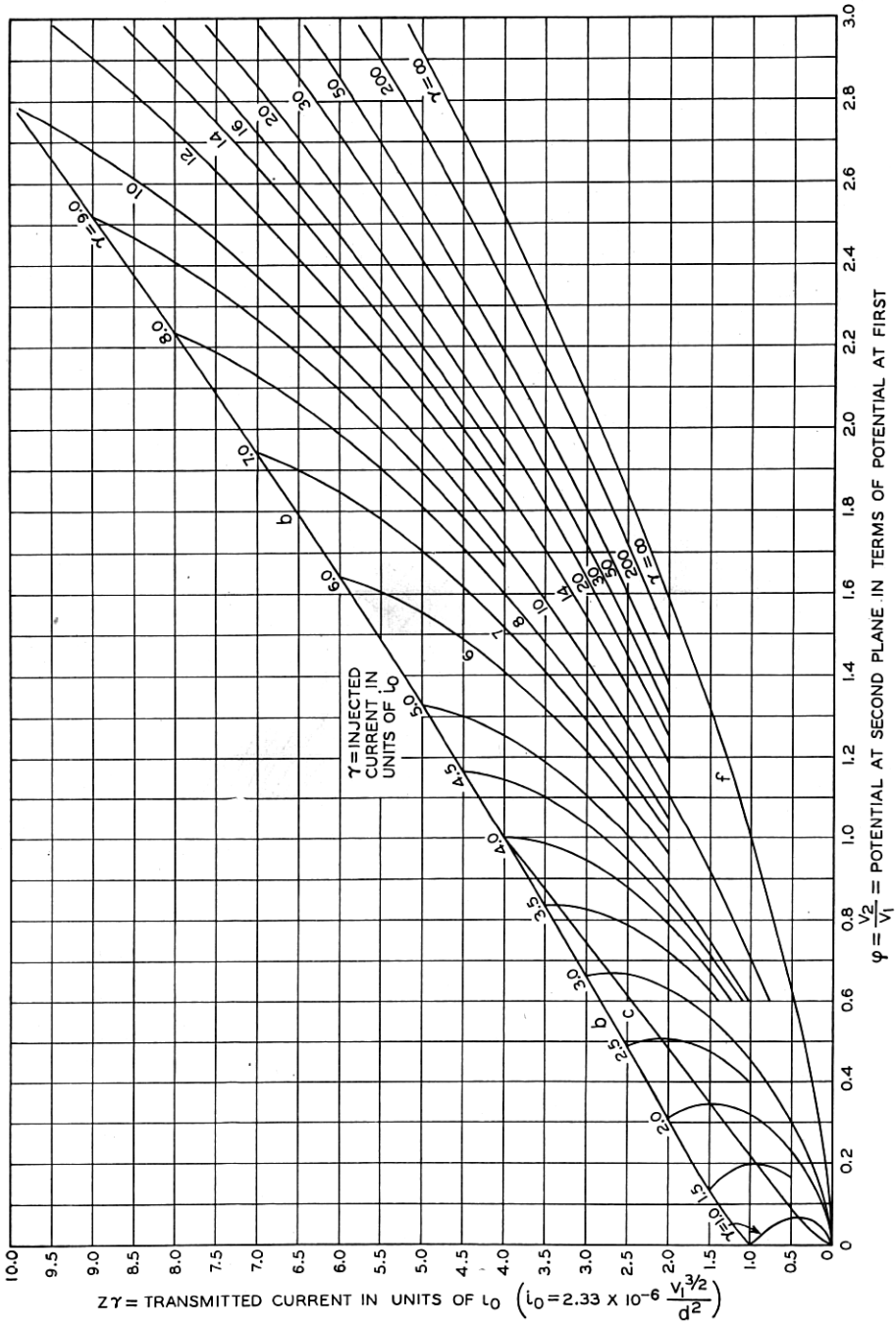

Fig. 9*a*—Electrical characteristics for type B distributions.

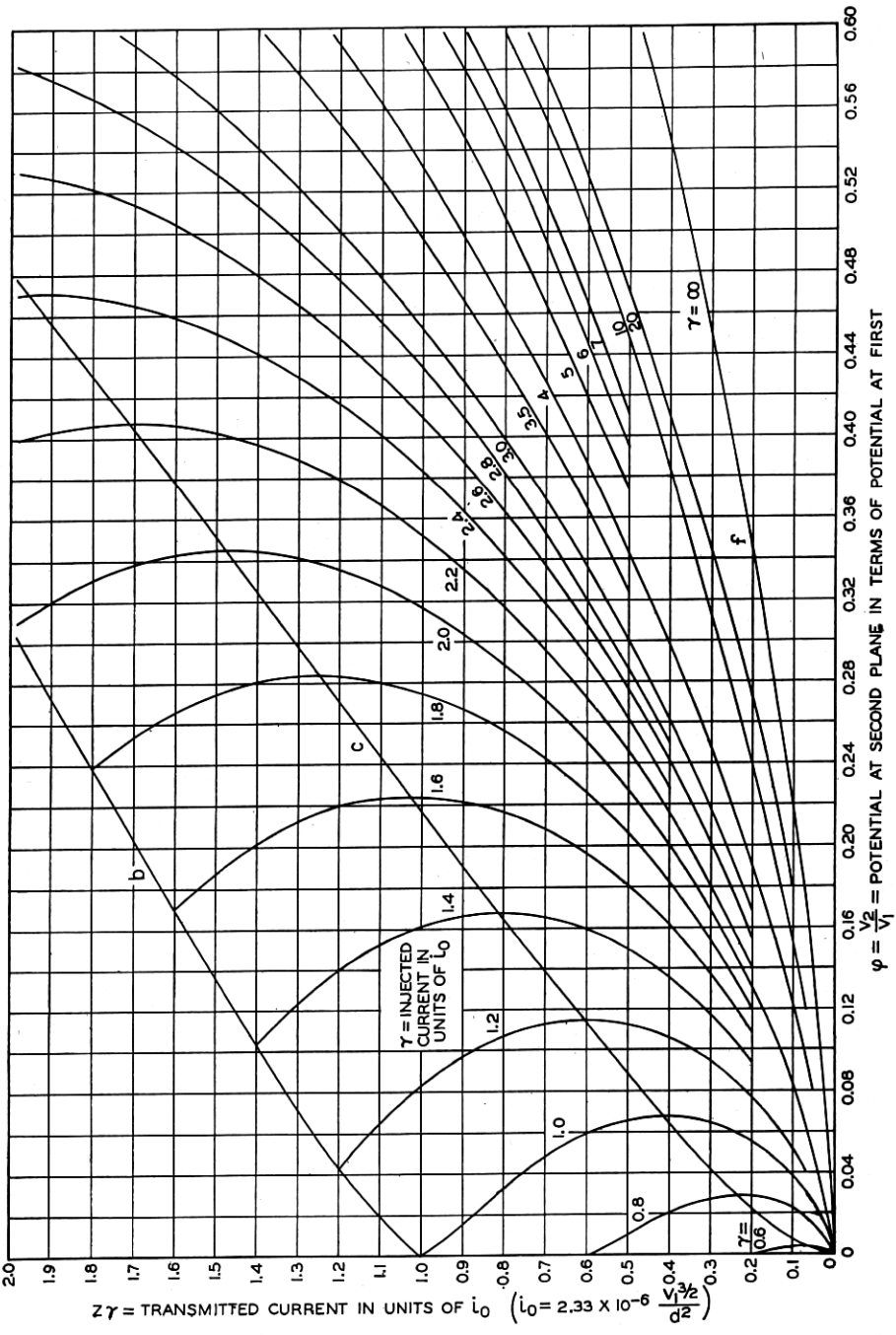

Fig. 9*b*—Enlargement of a portion of Fig. 9*a*.

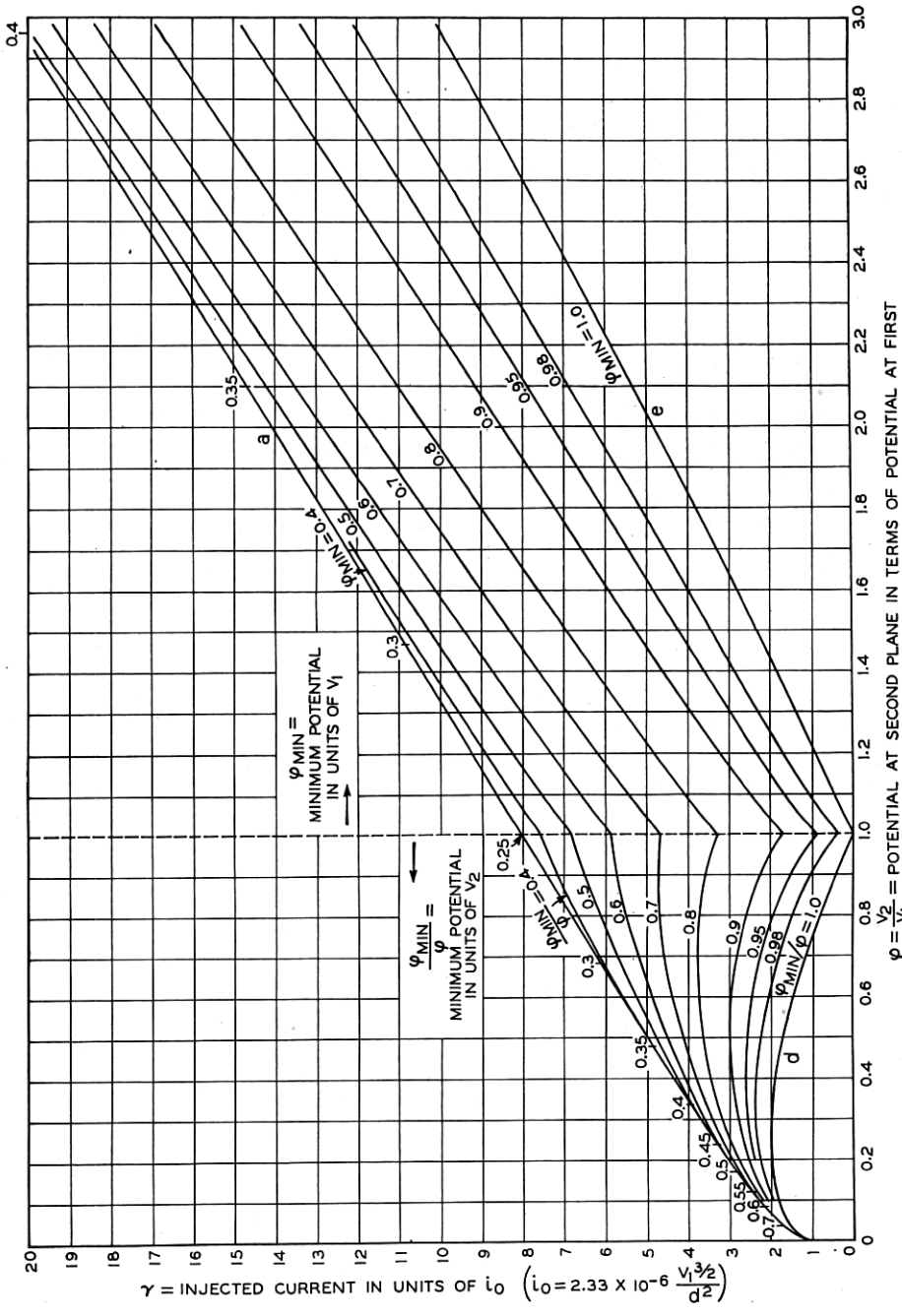

Fig. 10*a*—Electrical characteristics for type C distributions (overlap solutions on Fig. 11).

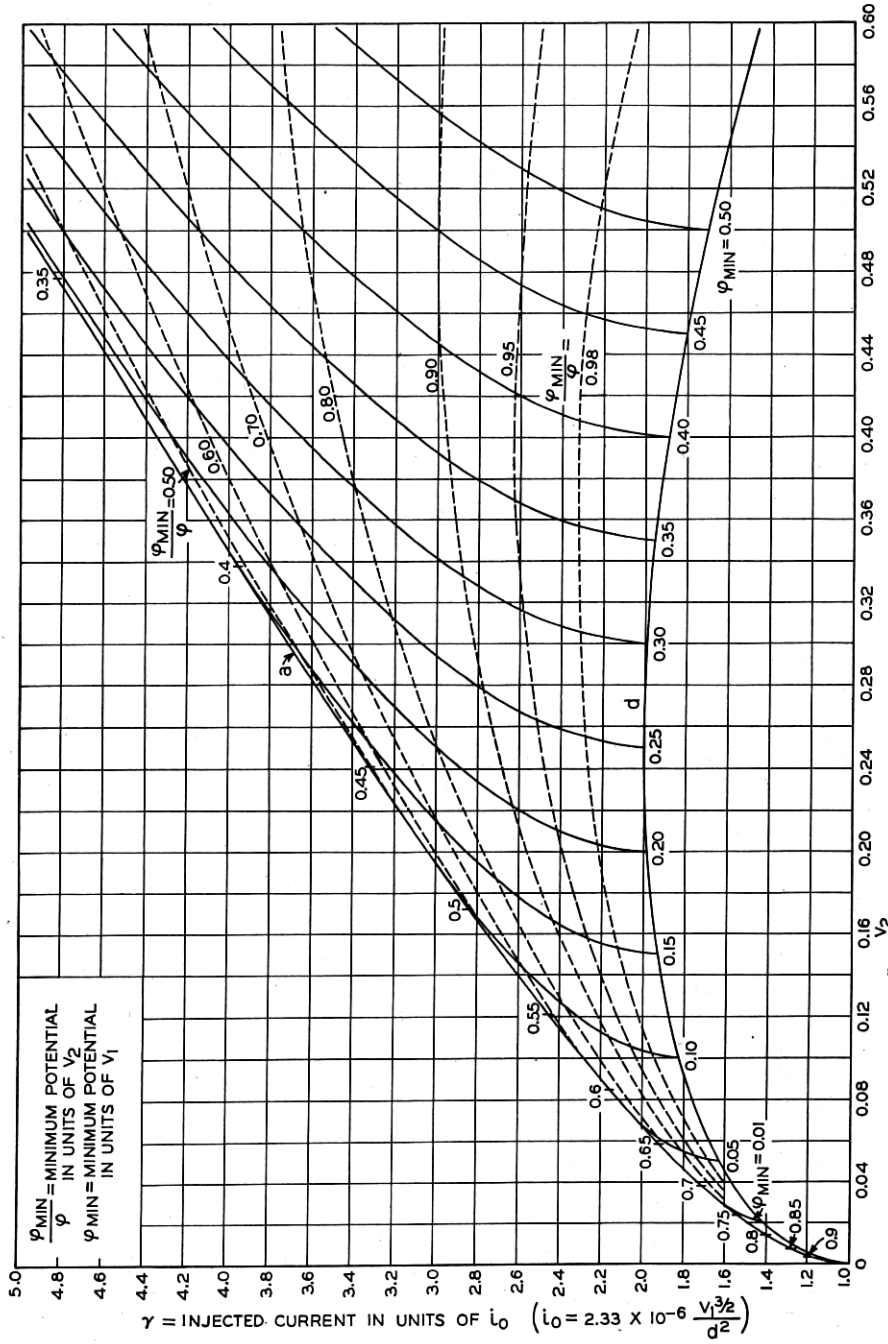

Fig. 10*b*—Enlargement of a portion of Fig. 10*a*.

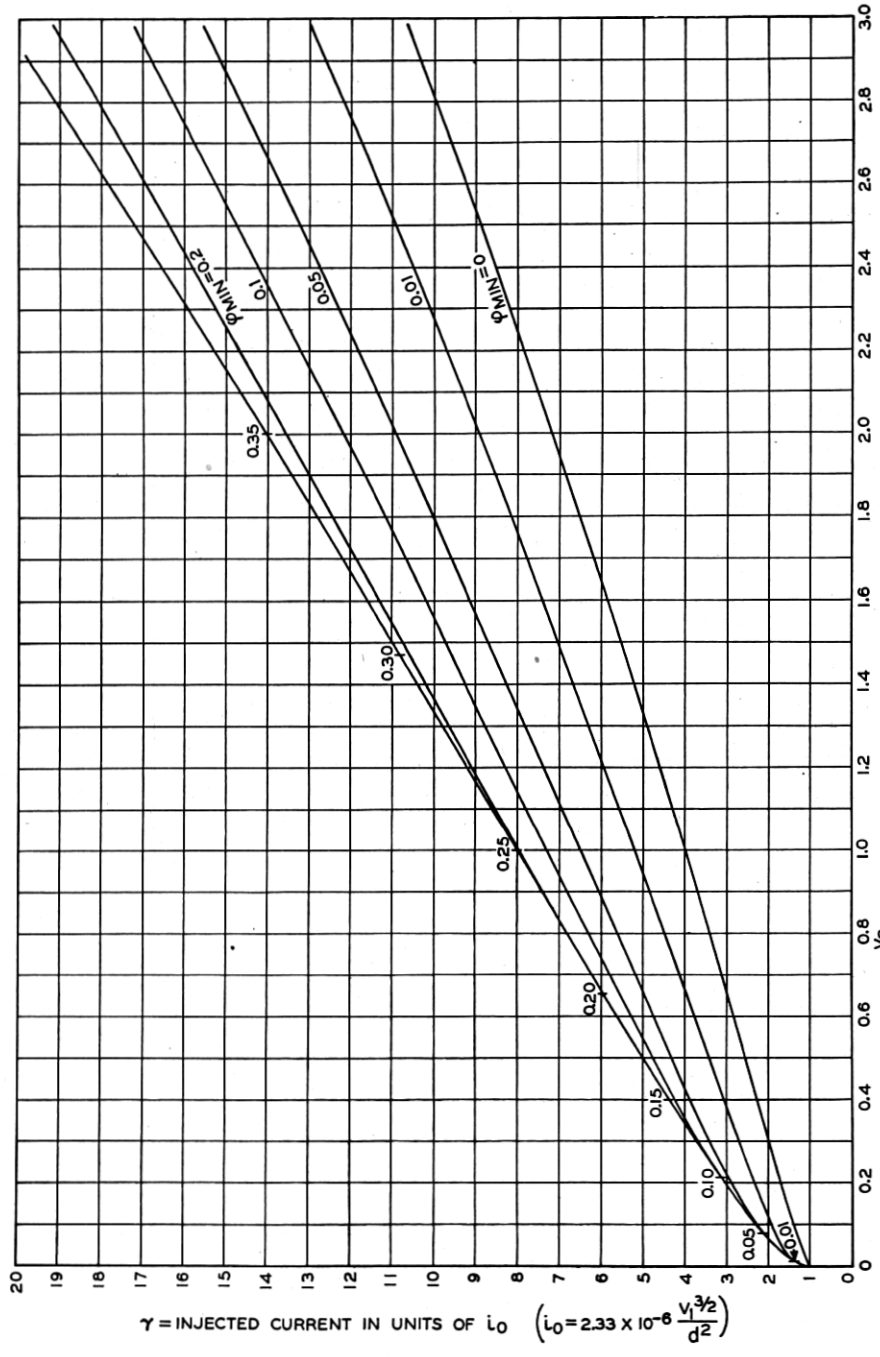

Fig. 11—Electrical characteristics for type C overlap distributions.

rises, finally reaching the limiting values indicated on the upper curve of Fig. 11; the limiting conditions there are precisely the same as for curve *a* of Fig. 10. Further increase of injected current produces a transition to type *B* solutions.

It seems questionable that this overlap type C condition can exist in a practical case. An investigation of this question involving external circuit considerations is beyond the scope of this paper.

Transition Between Distribution Types

The physical choice between the different possible potential distributions which may exist with a given set of boundary conditions is determined by the sequence in which the boundary conditions are established. Extreme values of any parameter are seen from Figs. 7 and 8 to lie in regions for which only one solution is possible. If the boundary conditions are varied slowly and continuously from these values, the indicated type of distribution will persist until the limit of this region is reached at which time a sudden transition must occur to another indicated type of distribution. Inspection of Figs. 7 and 8 will show that at such transitions only one other type of distribution is ever possible. The determination of the correct physical distribution can thus be made without ambiguity.

Certain peculiarities are, however, to be noted. A survey of all possible transitions in which γ and φ are treated as independent variables will indicate that, starting from extreme conditions and changing conditions continuously in the same direction, distributions of the overlap C type shown in Figs. 4 and 11 never occur. A second peculiarity has to do with the unstable region of type B solutions shown on Fig. 9. When this region is entered with insufficient resistance in the external circuit, instability results with a sudden transition to a corresponding stable type of distribution.

The space model shown in Fig. 12 has been found to be of value in visualizing problems involving transitions. The three coordinates used in its construction are the second electrode potential φ (to the right) the injected current γ (to the left) and the transmitted current $Z\gamma$ (vertical). Solutions corresponding to potential distributions of the C and D type, for which $Z\gamma = \gamma$, appear as a celluloid plane inclined at 45 degrees, on which the values of the potential minima are indicated. Solutions of the C overlap type have been omitted. Solutions of the B type are represented by the concave surface of the model. Viewing the model from a different angle as shown in Fig. 13 (where the celluloid sheet is removed) the unstable B region appears as an over-hanging cliff extending between γ values of 0.5 and 4. Bounding curve *c*

separating the unstable region from the stable region is drawn on the model and lies along the vertical surface of the cliff. The small region lying between γ values of 0 and 0.5, for which direct transitions between A solutions and D solutions occur, can be seen in both views as a small vertical cliff.

Solutions corresponding to varying conditions will be given by the position of a movable particle confined to the surface of the model.

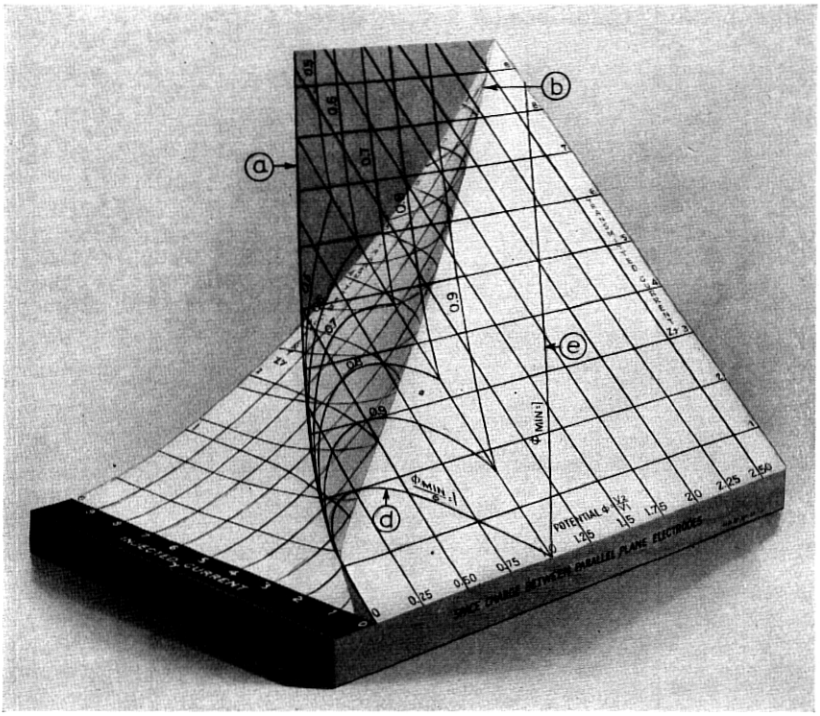

Fig. 12—A three-dimensional model illustrating the current-voltage relationships. Solutions of types C and D appear on the celluloid surface and solutions of the B type appear on the concave surface.

When this particle lies on the celluloid surface it may be moved around at will and will not "fall off" unless an attempt is made to go to larger values of the injected current γ than is permitted by the bound-curve a (the curved edge of the celluloid). The particle may, however, "fall off" at this edge and land on the concave surface from which it can escape only by climbing up the surface to the bounding curve b which is common to both surfaces. The overhanging cliff is, however, particularly treacherous, for unless the particle is supported by the

existence of sufficient resistance in the circuit connected to the second electrode, it will go through the model coming to rest on the celluloid surface above. With no resistance in the external circuit this curious behavior will occur at the vertical part of the cliff indicated by the bounding curve *c*. The presence of some resistance will cause this to occur for larger values of $Z\gamma$. The exact place can of course be determined by noting the point of tangency between a resistance line drawn on Fig. 9 and one of the characteristic curves—just as the stable operating conditions for any negative resistance device is found.

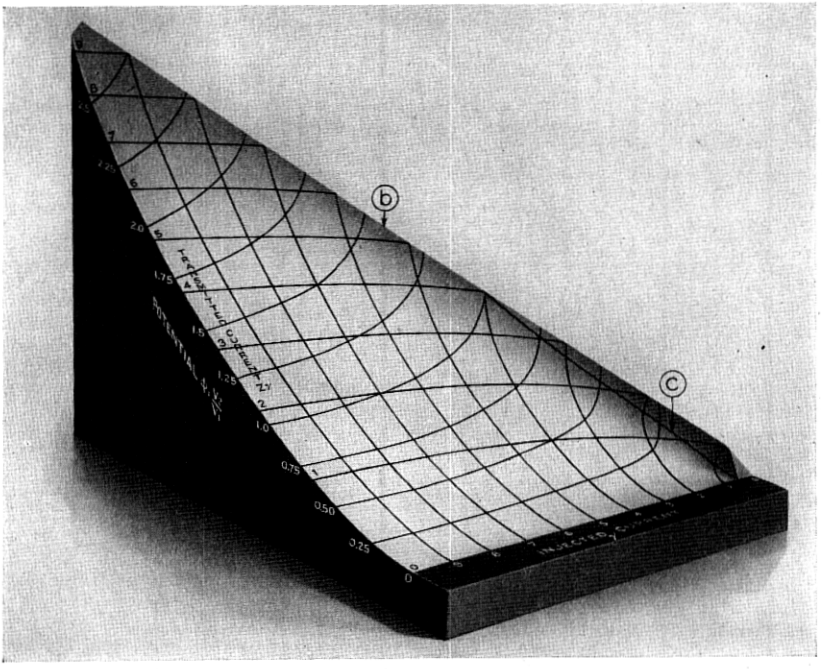

Fig. 13—A different view of the concave surface of the model shown in Fig. 12. (The celluloid surface has been removed.)

The entire surface is stable if the external resistance is greater than approximately 0.25 in units of $\varphi/Z\gamma$.

Illustrative Examples

I. Class B Operation of a "Critical Distance" Tetrode

Since the purpose of "critical distance" operation is to prevent the passage of secondary electrons from the plate (our second plane) to the screen grid (our first plane), the existence of a potential minimum

is desired; however, type B solutions with some reflected electrons would be objectionable. The permissible operating range must therefore lie in the C region on Fig. 7. If, for example, we operate the tube with $V_2 = V_1$ as the quiescent point and with a resistance load, the operating curve is a straight line through the point $\gamma = 0$, $\varphi = 1$. The upper excursion of this line is set by the upper limit, curve a, of the C region. For characteristics which cross curve d and enter the D region a loss of suppression would result. Maximum efficiency occurs with the largest possible excursion of V_2, that is for a line tangent to the d curve at the quiescent point. The minimum instantaneous value of V_2 for the conditions specified is seen to be 25 per cent of its quiescent value as contrasted with a usual value of about 10 per cent for a pentode when similarly operated. For the instantaneous value of V_2 to fall to 10 per cent of its initial value (without loss of suppression) the quiescent point must be at $\gamma = 0$, $\varphi = 1.3$ with the operating line tangent to curve d at about $\varphi = 0.5$. Operation in the D region above $\varphi = 1$ does not result in a secondary current from plate to grid.

II. Triode Operation in the Positive Grid Region

Figure 1 may be taken as representing an idealized triode. The second plane represents the plate so that $V_2 = V_p$ and the first plane represents the grid plane with effective potential V_1. We let

$$V_1 = V_g + V_p/\mu,$$

where μ will be a variable if space charge is formed in the plate-grid region and may differ considerably from its "cut-off" value.

If the fraction of the electrons stopped by the grid is negligible and if operation does not enter the B region, with disturbing effects produced by reflected electrons, then Fig. 1 becomes an accurate representation and in view of the choice of units σ is a geometrical constant of the tube. Hence the operating characteristic is a constant γ line ($\gamma = \sigma^2$) on Fig. 7.[19]

For normal operation the characteristic must not extend into the B region. If the grid is to be driven far positive it is desirable to stay in the C region for all values of $\varphi < 1$ to prevent secondary electrons from leaving the plate. The minimum value of φ as a function of γ may be read from the intersections of the constant γ lines with limiting curve a if $\gamma > 2$ and limiting curve d if $\gamma < 2$. Now since

$$\varphi = \frac{V_P}{V_1} = \frac{V_P}{V_g + \dfrac{V_P}{\mu}}$$

[19] Proof of the relationship $\gamma = \sigma^2$ is contained in the appendix.

and

$$V_g/V_P = \frac{1 - \varphi/\mu}{\varphi} = \frac{1}{\varphi} - \frac{1}{\mu},$$

if μ and σ are known, the maximum value of V_g/V_P may be calculated. Fig. 7 shows that a value of γ just greater than 2 will give the lowest minimum value for φ ($\varphi = 0.07$) by intersection with curve a. In this region $\varphi/\mu \ll 1$ so that

$$\left(\frac{V_g}{V_P}\right) \text{max.} = \frac{1}{\varphi} = 14.$$

For values of γ only slightly less than 2 the minimum value of φ rises abruptly, being given by the intersection with curve d, while for values greater than 2 the rise in φ is not so abrupt.

It should be noted that for the usual cylindrical triode the departure from the parallel plane case is not very marked in the grid-plate region while it can be taken into account by the usual cylindrical formulæ for the cathode grid region. It therefore becomes possible to extend this analysis in an approximate sort of way to cover the cylindrical case.

APPENDIX

Definition of Symbols

V_1 = Potential of the first plane in volts,
V = Potential of a second plane in volts,
φ = Ratio of the potential at the second plane to the potential of the first plane,
I = Injected current in amperes per sq. cm.,
x = Distance in centimeters,
d = Spacing between the two planes in centimeters (used when this distance is regarded as a fixed quantity),
S = Distance between the two planes in centimeters (used when this distance is regarded as a variable),
σ = Distance between the planes expressed in units S_0,

$$S_0 = 1.527 \times 10^{-3} \frac{V_1^{3/4}}{I^{1/2}} \text{ (centimeters)},$$

$$a = 1.527 \times 10^{-3} = [10^{13}(2e/mc)^{1/2}/9\pi c^2]^{1/2},^{20}$$

$a^2 = 2.33 \times 10^{-6}$,
Z = Fraction of the injected current I which reaches the second plane,
t = Time in seconds,
T = Electron transit time between the planes in seconds,

τ = Electron transit time expressed in units of t_0,

$t_0 = 7.72 \times 10^{-11} \dfrac{V_1^{1/4}}{I^{1/2}}$ (seconds),

$c = 7.72 \times 10^{-11} = 3a(m\mathbf{c}/2e)^{1/2}10^{-4}$,[20]

γ = Injected current expressed in units of i_0,

$i_0 = 2.33 \times 10^{-6} \dfrac{V_1^{3/2}}{d^2} = \dfrac{a^2 V_1^{3/2}}{d^2}$ (amperes per sq. cm.),

α = Ratio of the potential at a potential minimum when one exists to the potential of the first plane, otherwise merely a convenient constant of integration. (In the text the symbol $\varphi_{min.}$ is used in the cases where the physical significance can be attached.)

β = An integration constant similar to α but associated with an opposite sign.

Relationship between γ and σ

By definition

$$S_0 = \frac{a V_1^{3/4}}{I^{1/2}} = \frac{S}{\sigma} \tag{1}$$

and

$$i_0 = \frac{a^2 V_1^{3/2}}{d^2} = \frac{I}{\gamma}. \tag{2}$$

Solving (1) for σ

$$\sigma = \frac{S I^{1/2}}{a V_1^{3/4}}. \tag{3}$$

Solving (3) for γ

$$\gamma = \frac{d^2 I}{a^2 V_1^{3/2}}. \tag{4}$$

But since $S = d$ for the conditions under which γ is used

$$\gamma = \sigma^2 \tag{5}$$

Derivations

The space charge equation based upon Poisson's equation and the energy equation for an electron is[21]

$$\frac{d^2 V}{dx^2} = \frac{4}{9a^2} I V^{-1/2}. \tag{6}$$

[20] In this work e is the charge on the electron in e.s.u., m its mass in grams, $\mathbf{c}$ is the ratio of electrostatic and electromagnetic units, 1 volt = $(10^8/\mathbf{c})$ e.s.u., 1 ampere = $(\mathbf{c}/10)$ e.s.u.

[21] See, for example, Dow, "Fundamentals of Engineering Electronics," John Wiley, 1937, pg. 100.

This implies that all of the electrons at any plane have the same speed, a condition which must be borne in mind when the present analysis is applied.

Integration of equation (6) yields

$$\left(\frac{dV}{dx}\right)^2 = \frac{16}{9}\frac{I}{a^2}(V^{1/2} + \text{const.}) \tag{7}$$

The choice of zero for this constant leads to type B distributions. A negative constant gives type C distributions, and some of the type D distributions while a positive value gives type A and type D distributions. These will be considered in detail in the sections which follow.

Transit time solutions are obtained by writing the energy equation for an electron in a conservative field which in practical units is

$$\frac{dx}{dt} = \left(\frac{2eV10^8}{mc}\right)^{1/2} = \frac{3a}{c}V^{1/2}. \tag{8}$$

Solving for t and introducing numerical values

$$t = \int \frac{c}{3a}V^{-1/2}\,dx = 1.68 \times 10^{-8}\int V^{-1/2}dx \tag{9}$$

$$= 1.68 \times 10^{-8}\int \left(\frac{dV}{dx}\right)^{-1} V^{-1/2}dV.$$

Specialization of this equation for the various types is carried out below.

Integration Constant Zero—Type B

If the constant in equation (7) is set equal to zero, the next integration gives Child's equation, applicable to the type B distribution when the correct values of current are used, corresponding to conditions before and after the potential zero. Before the potential zero the total current, i.e., the arithmetic sum of injected and reflected currents, is $(2 - Z)I$ so that

$$(2 - Z)I = \frac{a^2V^{3/2}}{x^2}, \tag{10}$$

where V is the potential x centimeters before the zero. Hence measuring distance from the first plane in units of S_0 and expressing potential in units of V_1,

$$\sigma_- = \frac{1}{(2 - Z)^{1/2}} - \frac{\varphi^{3/4}}{(2 - Z)^{1/2}}. \tag{11}$$

Similar analysis for the region beyond the potential zero where

$$ZI = \frac{a^2 V^{3/2}}{x^2}, \tag{12}$$

yields

$$\sigma_+ = \frac{1}{(2 - Z)^{1/2}} + \frac{\varphi^{3/4}}{Z^{1/2}}. \tag{13}$$

Introducing the identity $\gamma = \sigma^2$ in equation (13) gives the relationship

$$Z\gamma = \left[\left(\frac{Z}{2 - Z} \right)^{1/2} + \varphi^{3/4} \right]^2. \tag{14}$$

Some of the limiting curves associated with the B solutions are closely related, as is implied by the use of a common letter. Curve c in Fig. 2 corresponds to maximum values of φ for fixed values of σ and hence of $\gamma = \sigma^2$. By inspection this is seen to be the same condition as is implied by curve c in Fig. 9. To find these curves we make φ a maximum in (13) with respect to Z holding σ constant and obtain:

(c)
$$\begin{cases} Z = 2\varphi^{1/2}/(1 + \varphi^{1/2}), & (15) \\ \sigma = (1 + \varphi^{1/2})^{3/2} 2^{-1/2}. & (16) \end{cases}$$

From these the various other forms of curve c are readily found by the relationships $\gamma = \sigma^2$ and $Z\gamma = Z\sigma^2$. The curve b of Fig. 2 corresponds to $Z = 1$ and gives in equation (13)

(b)
$$\sigma = 1 + \varphi^{3/4}. \tag{17}$$

The minimum transmitted current for fixed φ, curve f in Figs. 8 and 9, is seen to correspond to $\gamma \to \infty$; for this the virtual cathode recedes to the first plane and

(f)
$$Z\gamma = \varphi^{3/2}. \tag{18}$$

Introducing dV/dx obtained from equation (7) with the correct current and a zero constant into equation (9) and integrating gives

$$T = \frac{cV^{1/4}}{(2 - Z)^{1/2} I^{1/2}} + \text{const.}, \tag{19}$$

which in units of t_0 measured from the first plane with potentials in units of V_1 gives

$$\tau_- = \frac{1 - \varphi^{1/4}}{(2 - Z)^{1/2}}. \tag{20}$$

Similar analysis to points beyond the potential zero yields

$$\tau_+ = \frac{1}{(2 - Z)^{1/2}} + \frac{\varphi^{1/4}}{Z^{1/2}}. \tag{21}$$

Integration Constant Negative—Types C and D

Introducing for the constant in equation (7) a negative value, say $-(\alpha V_1)^{1/2}$, will give a positive value of V (equal to αV_1) for $dV/dx = 0$ with $d^2V/dx^2 > 0$ and must therefore lead to solutions of the C type.

Integrating once more and introducing the unit S_0 gives

$$x = \pm S_0(\varphi^{1/2} + 2\alpha^{1/2})\sqrt{\varphi^{1/2} - \alpha^{1/2}} + \text{const.} \tag{22}$$

Expressing distance from the first plane in units of S_0, we find two possibilities:

$$\sigma_D = +(\varphi^{1/2} + 2\alpha^{1/2})\sqrt{\varphi^{1/2} - \alpha^{1/2}} - (1 + 2\alpha^{1/2})\sqrt{1 - \alpha^{1/2}} \tag{23}$$

and

$$\sigma_- = -(\varphi^{1/2} + 2\alpha^{1/2})\sqrt{\varphi^{1/2} - \alpha^{1/2}} + (1 + 2\alpha^{1/2})\sqrt{1 - \alpha^{1/2}}. \tag{24}$$

The first of these solutions gives a potential distribution rising continuously as σ increases from zero, hence of type D as was anticipated by the subscript. The second solution decreases to a minimum at

$$\sigma_{min.} = (1 + 2\alpha^{1/2})\sqrt{1 - \alpha^{1/2}} \tag{25}$$

and then increases, the equation to the right of the minimum being

$$\sigma_+ = (\varphi^{1/2} + 2\alpha^{1/2})\sqrt{\varphi^{1/2} - \alpha^{1/2}} + (1 + 2\alpha^{1/2})\sqrt{1 - \alpha^{1/2}}. \tag{26}$$

Curves given by equations 23, 24 and 26 are drawn in Fig. 3. If values of σ and φ corresponding to conditions on the boundary planes are entered in the figure, a C solution is indicated only if the point falls upon a curve of the σ_+ type. This curve then gives the potential distribution to the right of the minimum; to the left of the minimum the distribution is given by the σ_- curve with the same value of α, which has the interpretation $\alpha = \varphi_{min.}$ for this case. Points entered on the σ_- or σ_D curves will clearly give D type solutions.

Three equations for limits of the C region can easily be written down on the basis of the above equations:

(b) $$\sigma = 1 + \varphi^{3/4}. \tag{27}$$

(d) $$\sigma = (1 + 2\varphi^{1/2})\sqrt{1 - \varphi^{1/2}}. \tag{28}$$

(e) $$\sigma = (\varphi^{1/2} + 2)\sqrt{\varphi^{1/2} - 1}: \tag{29}$$

The curve a is obtained by making σ_+ a maximum with respect to α while holding φ constant. This gives

(a)
$$\begin{cases} \alpha = \varphi_{min.} = \varphi(1 + \varphi^{1/2})^{-2}, & (30) \\ \sigma = (1 + \varphi^{1/2})^{3/2}. & (31) \end{cases}$$

Here φ and σ are coordinates of a point on the a curve and $\alpha = \varphi_{\min.}$ is the parameter value for the potential distribution curve tangent to curve a at that point. The σ_+ curves give type C solutions for values before the tangent point and give C overlap solutions beyond this point.

All the curves described in this section are readily transformed to current voltage plots by the relationships $\gamma = Z\gamma = \sigma^2$.

The transit times for the various curves are found from equations (7) and (9) using the value $-(\alpha V_1)^{1/2}$ for the constant. Integrating and measuring time from the first plane, they are

$$\tau_D = +(\varphi^{1/2} - \alpha^{1/2})^{1/2} - (1 - \alpha^{1/2})^{1/2}. \quad (32)$$

$$\tau_{c-} = -(\varphi^{1/2} - \alpha^{1/2})^{1/2} + (1 - \alpha^{1/2})^{1/2}. \quad (33)$$

$$\tau_{c+} = +(\varphi^{1/2} - \alpha^{1/2})^{1/2} + (1 - \alpha^{1/2})^{1/2}. \quad (34)$$

Integration Constant is Positive—Type D

Type D solutions include those given by equations (23) and (24).

Other solutions are obtained by giving the integration constant of equation (7) a positive value, say $+(\beta V_1)^{1/2}$. Integrating the equation and measuring distances from the first plane in units of S_0 we obtain the two possibilities:

$$\sigma = +(\varphi^{1/2} - 2\beta^{1/2})\sqrt{\varphi^{1/2} + \beta^{1/2}} - (1 - 2\beta^{1/2})\sqrt{1 + \beta^{1/2}}, \quad (35)$$

which applies for $\varphi > 1$, and

$$\sigma = -(\varphi^{1/2} - 2\beta^{1/2})\sqrt{\varphi^{1/2} + \beta^{1/2}} + (1 - 2\beta^{1/2})\sqrt{1 + \beta^{1/2}}, \quad (36)$$

which applies for $\varphi < 1$. Corresponding transit times are:

$$\tau = +(\varphi^{1/2} + \beta^{1/2})^{1/2} - (1 + \beta^{1/2})^{1/2}. \quad (37)$$

$$\tau = -(\varphi^{1/2} + \beta^{1/2})^{1/2} + (1 + \beta^{1/2})^{1/2}. \quad (38)$$

Integration Constant is Positive—Type A

The potential distribution curves of the A type are identical in form with those of the D type, where $\varphi < 1$, which result from the

positive value of the constant in equation (7). They differ in numerical values in that the current I must be replaced by the value $2I$ to allow for the reflected current. The correct equation is then

$$\sigma = [(1 - 2\beta^{1/2})(1 + \beta^{1/2})^{1/2} - (\varphi^{1/2} - 2\beta^{1/2})(\varphi^{1/2} + \beta^{1/2})^{1/2}]2^{-1/2}. \quad (39)$$

The corresponding transit times are given by

$$\tau = [(1 + \beta^{1/2})^{1/2} - (\varphi^{1/2} + \beta^{1/2})^{1/2}]2^{-1/2}. \quad (40)$$

To the right of $\varphi = 0$ the space is free of charge so that the potential gradient is constant and equal to the value at $\varphi = 0$ obtained by taking the derivative of equation (39). This value is

$$\frac{d\varphi}{d\sigma} = -\frac{4\sqrt{2}\beta^{1/4}}{3}. \quad (41)$$

Concerning Completeness

We may now review our work and see that no possible space charge distributions can have been omitted. Starting from the fundamental equation (6) we obtain equation (7) with an undetermined integration constant. Setting this constant equal to zero we could integrate once more, obtaining a solution formally identical with Child's equation. If we supposed that the cathode plane defined by the Child's solution lay to the right of the initial plane, then the only freedom left in the solution was represented by Z, the fraction of current passing through the plane. All physically sensible values of Z, i.e., 0 to 1, are included in the solutions. If the cathode is assumed to lie to the left of the plane, then Z must equal 1 and the solution which arises is given by $\alpha = 0$ in equations (23) or (26), or $\beta = 0$ in equation (35)—that is, a D solution. For a negative value of the constant, a further integration gave only two possibilities. Each of these was investigated for all possible values of the constant. A similar statement is true for positive values of the constant.

As was stated in the text, space charge distributions corresponding to injection from both bounding planes can be handled in formally the same way as injection from one plane; therefore we may conclude that all solutions to the problem given by specifying the boundary conditions on two planes, subject to the assumptions represented by equation (6), have been determined.

Equations for Boundary Curves

For convenience we append a table of equations for the limiting curves occurring in the figures.

Symbol	Equation numbers	σ	γ	Z	$Z\gamma$
a	31	$(1+\varphi^{1/2})^{3/2}$	$(1+\varphi^{1/2})^3$	1	$(1+\varphi^{1/2})^3$
b	17, 27	$1+\varphi^{3/4}$	$(1+\varphi^{3/4})^2$	1	$(1+\varphi^{3/4})^2$
c	15, 16	$(1+\varphi^{1/2})^{3/2}2^{-1/2}$	$(1+\varphi^{1/2})^3/2$	$\frac{2\varphi^{1/2}}{(1+\varphi^{1/2})}$	$\varphi^{1/2}/(1+\varphi^{1/2})^2$
d	28	$(1+2\varphi^{1/2})\sqrt{1-\varphi^{1/2}}$	$(1+2\varphi^{1/2})^2(1-\varphi^{1/2})$	1	$(1+2\varphi^{1/2})^2(1-\varphi^{1/2})$
e	29	$(\varphi^{1/2}+2)\sqrt{\varphi^{1/2}-1}$	$(\varphi^{1/2}+2)^2(\varphi^{1/2}-1)$	1	$(\varphi^{1/2}+2)^2(\varphi^{1/2}-1)$
f	18	∞	∞	0	$\varphi^{3/2}$

The further relationship

$$\alpha = \varphi_{\min.} = \varphi(1+\varphi^{1/2})^{-2} \tag{30}$$

holds for the a curve.